Kinetic analysis of gluconate phosphorylation by human gluconokinase using isothermal titration calorimetry

Neha Rohatgi[1,2], Steinn Guðmundsson[1] and Óttar Rolfsson[1,2*]

[1]Center for Systems Biology, University of Iceland, Sturlugata 8, 101 Reykjavik, Iceland.
[2]University of Iceland Biomedical Center, Laeknagardur, 101 Reykjavik, Iceland

*Corresponding Author

Running title: Characterization of human GntK

Key words: Enzyme kinetics, Isothermal titration calorimetry, Gluconate (Glcn), Human gluconokinase (hGntK, IdnK), Human metabolism

Contact Information:
Óttar Rolfsson
ottarr@hi.is,
telephone: +354-8450075
Center for Systems Biology
University of Iceland
Sturlugata 8
101 Reykjavik
Iceland

Abstract

Gluconate is a commonly encountered nutrient, which is degraded by the enzyme gluconokinase to generate 6-phosphogluconate. Here we used isothermal titration calorimetry to study the properties of this reaction. ΔH, K_M and k_{cat} are reported along with substrate binding data. We propose that the reaction follows a ternary complex mechanism, with ATP binding first. The reaction is inhibited by gluconate, as it binds to an Enzyme-ADP complex forming a dead-end complex. The study exemplifies that ITC can be used to determine mechanisms of enzyme catalyzed reactions, for which it is currently not commonly applied.

Introduction

Gluconate (Glcn) is a naturally occurring carboxylic acid that is found abundantly in various fruits, vegetables and dairy products as well as being added to processed foods and pharmaceuticals due to its refreshing taste. Gluconate has also found use in formulation chemistry, both in industry and in the health sector on account of its metal chelating properties. In the clinic, calcium gluconate is used for treating calcium deficiency, hydrofluoric acid burns and as dietary supplements in the form of zinc gluconate and iron gluconate derivatives [1, 2]. Despite widespread use of the compound across diverse sectors and its presence in human bio-fluids [3, 4] the details of gluconate production and consumption in humans remain relatively unexplored as highlighted in a recent metabolic network gap analysis of human metabolism [5].

Phosphorylated gluconate is an intermediate of the pentose phosphate pathway. The oxidation of 6-phosphogluconate contributes to NADPH formation in the cytosol and thus to both anabolic reactions and the recycling of glutathione, ultimately combating oxidative stress [6, 7]. Metabolism of gluconate is likely to follow this pathway given that consumed gluconate is absorbed and subsequently phosphorylated (**Fig. 1**). Indeed, isoform I of the human gene C9orf103 was recently shown to encode gluconokinase activity [5]. Through a computational metabolic modeling approach, the metabolic contribution of gluconate has also been estimated to have broad impact on cellular metabolism in accordance with its contribution to NADPH formation [8]. It is likely that gluconate follows this metabolic route in humans. Early biochemical investigations into the fate of gluconate added to rat liver perfusions strengthen this hypothesis. These studies showed that gluconate is internalized but is metabolized differently as compared to glucose [9]. In addition, gluconate metabolism in prokaryotes and lower eukaryotes is very well characterized where it is metabolized following phosphorylation by gluconokinase [10]. The biological conditions under which human gluconokinase (hGntK) is active have not been deduced. Analysis of publically accessible gene expression profiles indicate that these are likely context specific with the gene primarily expressed in brain, lymph node, kidney and hepatic tissue. Despite incomplete understanding of its metabolic context, human gluconokinase activity is encoded within the human genome and this enzyme is likely to play a pivotal role in the metabolism of gluconate in humans.

Gluconokinase belongs to the family of FGGY carbohydrate domain containing kinases [11] of which gluconokinase from *Escherichia coli* is one of the best described [12-14]. We recently reported the biochemical characterization of a recombinantly produced isoform I of human gluconokinase (hGntK) encoded by the gene IDNK (Uniprot id: Q5T6J7). Human gluconokinase is a dimer, each monomer weighing 23.33 kDa, that catalyzes ATP dependent phosphorylation of gluconate to 6-phosphogluconate. The enzyme was shown to be similar in secondary structure to its *Escherichia coli* counterpart and was specific towards the phosphorylation of gluconate. The kinetics of the enzymatic reaction was characterized spectrophotometrically by coupling 6-phosphogluconate formation with consumption by 6-phosphogluconate dehydrogenase.

Here we report the kinetic characterization of the gluconokinase catalyzed reaction using isothermal titration calorimetry (ITC). The kinetic and thermodynamic characterization of metabolic enzymes has recently gained interest from the computational metabolic modeling community where kinetic parameters are required for models that accurately capture genotype/phenotype relationships [15]. Employing ITC we were able to study the reaction without any coupling of the reaction or tagging of the substrates. ITC was used to determine kinetic parameters of the reaction under varying concentrations of each substrate. Kinetic data was fit to equations descriptive of relevant reaction models to deduce the reaction mechanism. The results suggest that the gluconokinase reaction follows a ternary complex mechanism and is inhibited at high concentrations of gluconate.

Materials and methods

Recombinant human gluconokinase was prepared as described previously [8]. Protein concentration was estimated using Beer-Lambert's Law from measured absorbance at 280 nm. Molar absorption coefficient was calculated using Tyr, Trp and Cys content of the protein [16]. MicroCal iTC200 (MicroCal, Northampton, MA, USA) was used to monitor enzymatic activity

directly by detecting heat flow during the reaction at 25 ˚C. All the experiments were performed in a kinase assay buffer composed of 100 mM sodium phosphate, 40 mM NaCl, 2.5 mM $MgCl_2$ (unless otherwise stated) and at pH 7.2. All enzyme and substrate solutions were prepared in this buffer, in order to minimize the heat of dilution during injection. The reaction cell was filled with 200 µL of the reaction mixture, with stirring speed 1000 rpm and each reaction had an initial delay of 60 seconds. All the experiments were performed in triplicates. These assays were based on the principles of implementations of ITC described by Wiseman et al. [17]. The raw ITC data was analyzed using the MicroCal iTC200 Origin Software package and MATLAB (Mathworks, Natick, MA, USA) was used for fitting and plotting the data.

Determination of enthalpy change (ΔH)

We measured the enthalpy using the multiple injection ITC method [18, 19]. The experiment was carried out by titrating 0.7 µL of 20 mM Glcn into the reaction cell containing 33.5 nM hGntK and 1 mM ATP, at 40 minute intervals. A total of 20 injections were done which continued for 13 hours. The enthalpy of the reaction (ΔH) was then determined by dividing total heat change in each injection by the amount of substrate in the cell after the injection.

$$\Delta H = \frac{1}{[S]_{Total} \cdot V} \int_{t=0}^{t=\infty} \frac{dQ(t)}{dt} dt \qquad \text{[Eq 1]}$$

where $[S]_{Total}$ is the concentration of the limiting substrate, V is the volume of the reaction mixture and dQ is the heat change measured at time t. The determination of ΔH and the data fitting was done in MicroCal iTC200 Origin Software package for experiments performed at 25 and 37 ˚C. As after a few injections product concentration increased significantly and started affecting the rate, average of first few ΔH values was calculated [18]. For blanks, the substrate was injected in cell containing reaction mixtures without the enzyme and the blanks were then subtracted.

Kinetic experiments to study mechanism of reaction

ITC enables the determination of enzymatic parameters of the reaction under study as the rate of the reaction is proportional to the measured heat flow, according to:

$$\frac{dQ}{dt} = \frac{d[P]}{dt} \cdot V \cdot \Delta H \qquad \text{[Eq 2]}$$

In the experimental conditions where one substrate is at a saturating concentration, the enzymatic reaction can be described in terms of first-order kinetics in relation to the other substrate. The heat flow is given by:

$$\frac{dQ}{dt} = \Delta H V k \, [S]_0 \exp(-kt) \qquad \text{[Eq 3]}$$

where, k is the rate constant, and $[S]_0$ is the initial concentration of the limiting substrate, ΔH is the experimentally determined molar enthalpy for the reaction.

Kinetic parameters were determined under pseudo steady-state conditions [20]. The sample cell was loaded with a solution containing hGntK (67 nM) and a fixed concentration of Glcn. Sixteen injections of 1.5 µL (20 mM) ATP were done every 60 s at 25 ˚C. The saturating concentration of the fixed substrate is important for the estimation of kinetic parameters but for determining the mechanism, the fixed substrate has to vary over a broader range, from sub-saturated to saturated concentrations. Thus for these experiments, Glcn was fixed from 0.5 mM to 12.5 mM. As the concentration of ATP in the cell increases from 0.15 mM to 2.4 mM, the concentration of $MgCl_2$ was maintained at 6mM to maintain a steady amount of $MgATP^{2-}$. All experiments were done in triplicates or more. Analogous experiments were done for Glcn (20 mM), where 1.2 µL of Glcn was injected (16 injections) into the reaction solution containing 67 nM hGntK and 0.5 mM of fixed ATP concentration. The experiments for the other fixed ATP concentration values (1 mM – 7.5 mM) were performed at an enzyme concentration of 53.6 nM. The enzyme concentration in these experiments was reduced in order to attain a pseudo steady state condition after every injection. The $MgCl_2$ in these experiments was maintained at 5 mM excess of ATP. Enzyme blanks were carried out for each experiment. Reaction rates were obtained by dividing the measured baseline heat flow by the ΔH of the reaction (evaluated as described above). Primary plots for the kinetic data were plotted and analyzed in Origin.

Substrate Binding

Substrate binding experiments were performed to add more experimental support to the kinetic mechanism. For this, 36 injections of 1 µL of ATP (1 mM) were done every 120 seconds, in a cell containing 52.3 µM of hGntK. Similarly for Glcn, 36 injections of 1 µL (1 mM) were done every 120 seconds, in a cell containing 52.3 µM of hGntK. The basic principle behind these experiments is explained in detail in the book "Methods in cell biology" [21]. The heat change measured after every injection is proportional to the level of binding of the substrate to the enzyme. "Single Set of Identical Sites" model in the MicroCal iTC200 Origin Software was used to calculate change in enthalpy, change in entropy during binding and the binding constant. Experiments without enzyme in the cell were performed in order to get the blank values.

MicroScale Thermophoresis (MST) experiments were carried out with fluorescently labeled hGntK. MST is based on the principle that molecules move within a temperature gradient based on their charge, size and hydration shell, a property called thermophoresis. The movement is traced by measuring fluorescence. A fluorescent label (NT- 647) was covalently attached to the protein using NHS coupling using a Monolith NT Protein Labeling Kit (NanoTemper Technologies GmbH, Munich, Germany). Labeled hGntK was kept constant at 10 nM, while the concentration of the non-labeled ATP was varied between 3 mM – 0.09 µM. The assay was performed in an assay buffer with 0.05% Tween-20 and prepared in protein low-binding tubes. After a short incubation, the samples were loaded into MST NT.115 hydrophilic glass capillaries and the MST analysis was performed using the Monolith NT.115. Similar experiments were performed for measuring the binding of Glcn, where the concentration of the non-labeled Glcn was varied between 50 mM – 1.5 µM.

Data fitting to estimate the kinetic parameters

In order to calculate the kinetic parameters, reaction rates obtained from the kinetic experiments were fitted to relevant equations, using a nonlinear least-squares procedure in MATLAB. As

substrate inhibition by Glcn was observed, the data was fitted to a compulsory-order ternary complex mechanism with substrate inhibition equation [Eq 4] and substituted enzyme mechanism with substrate inhibition [Eq 5].

$$Rate\ (v_i) = \frac{k_{cat}E_0[A][G]}{K_{iA}K_{mG} + K_{mG}[A] + K_{mA}[G] + [A][G]\left(1 + \frac{[G]}{K_{siG}}\right)} \quad \text{[Eq 4]}$$

$$Rate\ (v_i) = \frac{k_{cat}E_0[A][G]}{K_{mG}[A] + K_{mA}[G]\left(1 + \frac{[G]}{K_{siG}}\right) + [A][G]} \quad \text{[Eq 5]}$$

In the above equations v_i (mM/s) is the reaction rate, k_{cat} is turnover number, E_0 is the initial enzyme concentration, [A] and [G] (mM) are concentrations of ATP and Glcn respectively, K_{mA} and K_{mG} (mM) are the Michaelis-Menten constants for ATP and Glcn respectively, K_{iA} (mM) is the dissociation constant of Enzyme-ATP (this was determined experimentally), and K_{siG} (mM) is a constant that defines the strength of inhibition. The equations are taken from Fundamentals of Enzyme kinetics [22]. The model having the smallest residual sum of squares is then selected as best fit. When analysis of the residuals does not reveal a significant difference between models, the model with the fewest number of parameters is chosen.

Results

Determination of Δ*H* at 25 and 37 ˚C

The amount of heat exchanged by the reaction system with the surroundings over time was measured using ITC [21]. A prerequisite for determining kinetic parameters using ITC was the determination of reaction enthalpy (Δ*H*). This was required in order to relate heat change, the parameter measured by ITC, to product/substrate concentration, allowing the reaction rate to be calculated through changes in concentration over time [Eq 1]. The heat flow (µcal/s) was measured as a function of time, following multiple injections of Glcn into the calorimeter cell containing the reaction mixture as described in the materials and methods section. **Fig. 2** shows a thermogram resulting from the injections of 0.7 µL of 20 mM Glcn, into the cell containing ATP (1 mM) and 33.5 nM of hGntK. Each injection resulted in an exothermic reaction as observed from a negative value of the heat flow. After complete consumption of Glcn, the heat flow returned to the baseline level, indicating that the substrate had been used up. The enthalpy change (Δ*H*) of the reaction was calculated under these experimental conditions, with the Origin Software. The average enthalpy change of first seven injections was -8.04 ± 1.09 kcal/mol at 25 ˚C. In similar manner, the Δ*H* of hGntK was also determined at 37 ˚C, a physiologically more realistic temperature. Δ*H* at 37 ˚C was measured to be -8.22 ± 0.15 kcal/mol, by injecting 1 µL of Glcn (20 mM) into the cell containing 1 mM ATP and 33.5 nM hGntK.

Kinetics of gluconate phosphorylation

In order to determine the rate of Glcn phosphorylation by hGntK, the heat flow was measured as a function of time under pseudo steady-state conditions. In order to maintain pseudo steady-state conditions in ITC, a large amount of the substrate is injected into the reaction cell containing much lower concentration of the enzyme, thus there is negligible depletion in substrate concentration and the reaction proceeds at a steady rate. This was achieved using a multiple injection method where either substrate (ATP or Glcn) at known concentrations was titrated into the reaction mixture at time intervals that prevented the titrated substrate being totally consumed. **Fig. 3A** shows the thermograms resulting from injections of ATP into the sample cell containing hGntK and Glcn at fixed concentrations, ranging from 0.5 to 12.5 mM. Upon titration with ATP, heat was initially consumed by the reaction mixture (heat of dilution), followed immediately by a drop in thermal power, with respect to the baseline, indicating heat released by the reaction mixture. The output then became steady, corresponding to the point at which the hGntK catalytic rate is at its maximum, up until additional ATP was titrated into the cell and a new rate maximum was achieved, as defined by altered substrate concentrations. Human GntK reaction rates following each injection were calculated from **Eq 2**. At Glcn a concentration of 0.5 mM, the rate of reaction decreased after a few injections of ATP. This was caused by depletion of Glcn in the reaction mixture. At all other Glcn concentrations, this effect was not observed and the reaction rate increased until maximum rate was achieved.

Analogous experiments were done to determine the kinetics of Glcn. Glcn was injected into the sample cell containing a solution of hGntK with a constant ATP concentration (**Fig. 3B**). Upon titration of Glcn, we observed smaller injection peaks associated with substrate dilution than compared to ATP injection. A subsequent drop in thermal power indicative of an increase in reaction rate followed immediately thereafter, but after only a few injections of Glcn, the rate of reaction was reduced. This reduction in reaction rate was observed at all constant ATP concentrations (**Fig. 3B**, lower panels) as opposed to when Glcn was kept constant (**Fig. 3A**, lower panels) and was indicative of reaction inhibition due to excess Glcn.

Mechanism of Glcn phosphorylation by hGntK

Bimolecular reactions can be catalyzed through two distinct molecular mechanisms. We used the substrate inhibition observed to differentiate between a ternary-complex mechanism and a substituted-enzyme mechanism. Thus there was no need to do product inhibition studies in order to differentiate between different mechanisms [22]. Hanes-Woolf plots were generated, where the ratio of substrate concentration to reaction rate [S]/V is plotted against substrate concentration [S]. **Fig. 4A** shows that for ATP injections at variable Glcn concentration, a linear trend is observed with lines having no common point of intersection. The Hanes-Woolf plot of kinetic data series for Glcn injections in **Fig. 4B** shows non-linear curves that all intersect at a single point. These figures confirm that the reaction is inhibited by Glcn [21]. Hanes-Woolf plots for both the substrates together suggest a ternary complex mechanism with ATP binding first and inhibited by Glcn. For Glcn to inhibit the reaction following a ternary complex mechanism it will have to bind to the ADP-Enzyme complex forming a dead-end ADP-Enzyme-Glcn complex. Intrinsically, this also means that 6-phosphogluconate is the first product to leave.

Substrate Binding

In order to add support to our hypothesis about the mechanism of the reaction we performed substrate-binding experiments. Employing ITC, ATP and Glcn were injected into the cell containing hGntK at a fixed concentration. The heat changes during binding were measured for each substrate and the binding constants were calculated. These experiments indicated that ATP binds to the free enzyme but due to low heat of interaction these experiments were not accurate enough for K_d measurements. Binding of Glcn to the free enzyme could not be confirmed using ITC experiments. Thus, in order to obtain an accurate measure of K_d, MST experiments were done.

In MST experiments the movement of fluorescently labeled enzyme was measured with ATP and Glcn. The K_d value for ATP measured by MST was 90.5 μM ± 9.5 μM. The binding for Glcn was again too low to obtain an accurate estimate be measured accurately. K_d for Glcn was estimated nearly equal to 1.6 ± 0.3 mM. This shows that Glcn has very low affinity for the free enzyme in absence of ATP. **Fig. 5 (A)** shows the thermogram of ATP from ITC and **Fig. 5 (B)** shows the graph of concentrations versus normalized fluorescence from MST. Figures for Glcn are not provided because the binding was too low. These results support the hypothesis that the reaction adheres to an ordered binding of substrates, with ATP binding first.

Data fitting to calculate kinetic parameters (K_M and k_{cat})

In order to calculate the kinetic parameters, the data was fitted to equations describing ternary complex and substituted enzyme complex reaction mechanisms [Eq 4 and 5]. By comparing the residual errors and parameter estimates it was concluded that the data better corresponded to a compulsory-order ternary complex mechanism with substrate inhibition [Eq 4]. This was also supported by Hanes-Woolf plots of the data. The estimated kinetic parameters are shown in **Tables 1 and 2**. The kinetic parameters at sub-saturated concentrations are not accurate but just an estimate as explained in materials and methods. These experiments were done to get the mechanism. As seen in **Table 1**, k_{cat} decreases with increasing constant Glcn when ATP is being injected into the cell. On the other hand with ATP being kept fixed at increasing levels, it remains un-changed when Glcn is being injected, as seen in **Table 2**. We also observed that K_{si}, which is a constant that defines the strength of inhibition by Glcn, increases with increasing ATP. Combined, this further supports inhibition by Glcn.

Discussion

Determining kinetic and thermodynamic properties of enzyme catalyzed reactions using ITC is fairly common but to the best of our knowledge, it has never been utilized to understand kinetics of a reaction beyond Michaelis-Menten mechanism of reaction. Here we have demonstrated that ITC can be used to get a complete understanding of kinetic properties of an enzyme catalyzed reaction, including the mechanism of reaction.

Determination of the change in enthalpy was a prerequisite for the determination of hGntK kinetic parameters with ITC [21]. In Fig. 2 the isotherm shows that the reaction peaks were not consistent in shape which indicates product inhibition. Therefore the average of first seven injections where the inhibition was not significant was used to estimate ΔH for fitting the kinetic data [18]. The ΔH of the reaction at 25 ˚C and 37 ˚C were indicative of an exothermic reaction as expected accompanying the hydrolysis of ATP. The enthalpy change observed at 37 ˚C was slightly higher than the enthalpy change at 25 ˚C. The measured enthalpy change was nearly -8

kcal/mol, which is similar to reactions catalyzed by other small molecule phosphotransferases such as yeast hexokinase (-10.75 to -12.18 kcal/mol) [23], serine/threonine phosphatase (-8.7 kcal/mol) and Ap4A hydrolase (-8.6 kcal/mol) [18] whose reaction enthalpies have been determined by ITC.

The mechanism of the enzyme catalyzed reaction was determined to be a compulsory-ordered ternary complex mechanism. A Hanes-Woolf plot for Glcn revealed that Glcn inhibited the reaction, as the plots were parabolic. Similar plots for ATP were straight lines that had no common point of intersection. These two graphs together are typically seen when reactions follows compulsory-ordered ternary complex mechanism and are inhibited by the second substrate, in this case Glcn [21]. We performed substrate-binding experiments to add more experimental support to the sequential binding kinetic mechanism. As the heat of interaction is too low in order to obtain an accurate measure of K_d we confirmed this data with additional experiments in microscale thermophoresis. Data from ITC and MST show that Glcn has very low to negligible binding to the free enzyme in the absence of ATP. These results confirm that the reaction likely adheres to a ternary complex mechanism with ATP binding first.

A structural study of GntK in *E.coli* revealed that the ATP binding site is accessible in the absence of Glcn, whereas, Glcn cannot bind in absence of ATP [14]. Collectively all this data serves to confirm the previously proposed structural similarity between human and *E.coli* GntK and furthermore that the catalytic mechanism of these two enzymes is similar, where ATP binding induces a conformational change required to allow gluconate to bind. As Glcn inhibits the reaction, it implies Glcn also binds to the ADP-Enzyme complex forming a non-productive complex. This suggests that 6-phosphogluconate is the first product to leave. **Fig. 6** shows the proposed mechanism of the reaction. Gluconokinase from *Pseudomonad* and *Schizosaccharomyces pombe* both have been reported to follow ternary complex mechanism [24, 25]. Additionally, *S. pombe* gluconokinase was reported to form E-ADP-Gluconate complex meaning it also has substrate inhibition [26]. However, while *S. pombe* gluconokinase was reported to have random order of substrate binding, our results indicate that human gluconokinase has sequential binding of substrates, by substrate binding studies.

Kinetic data for the enzyme under varying substrate concentrations was fitted **Eq 4** and **5** to get more evidence for the predicted model and to calculate the kinetic parameters. The K_M for ATP lies in the range 0.1 to 0.3 mM at varying concentrations of Glcn. Although when Glcn is 2 mM, there is a large error in the parameter estimates. The K_M of Glcn is in the range 0.2 to 0.3 mM. In this case the parameters at ATP 7.5 mM have huge error. The values of K_M's of substrates for the structurally similar FGGY carbohydrate kinases lie in the range of 0.1 to 0.3 mM at 37 ˚C although with exceptions, the K_M for L-fuculokinase is for example 1.4 mM. The value of K_M of ATP and Glcn for *E. coli* GntK is reported to be 0.123 mM and 0.04 mM respectively at 25 ˚C. Earlier we reported kinetic parameters of hGntK using spectrophotometric assays. The K_M for ATP in previous study was calculated to be 0.34 ± 0.01 mM and k_{cat} to be 9.5 ± 0.5 sec^{-1} at a Glcn concentration 1 mM. This is comparable to K_M and k_{cat} in this study at Glcn 1 mM, the values for which are 0.28 ± 0.11 mM and 9.75 ± 1.65 sec^{-1}. For Glcn however, the data do not correspond to our earlier study as the range of Glcn concentrations tested earlier was not high enough to detect substrate inhibition. The parameters for Glcn are therefore not comparable [8].

Holistic approaches to modeling the metabolic states of cells are rapidly moving from static stoichiometric models of metabolism to dynamic kinetic models. Computational biologists have expressed a shortage in detailed biochemical data for organisms of interest required to build context specific dynamic metabolic models required to explain complex genotype phenotype relationships [26]. In this respect elucidating the kinetic parameters of enzymes has recently gained increased importance and attention because the descriptive and predictive capabilities of these models are dependent upon accurate biochemical information [27, 28]. Spectroscopic techniques determine kinetic parameters, with the need to couple the enzyme or labeling the substrate. This is not required in ITC. Thus isothermal calorimetry has the advantage of determining enzymatic activity and thermodynamic parameters directly and simultaneously [29]. Knowledge of these parameters is the key to understanding bioenergetics of metabolism and is used increasingly to compute metabolic flux phenotypes [30, 31]. Here we have reported the kinetic and mechanism of reaction of isoform I of hGntK encoded by the gene IDNK that was recently highlighted to be incompletely characterized in a metabolic systems analysis of human metabolic reactions.

Authors contributions

NR designed the study, carried out the experiments, performed the data analysis and wrote the paper, SG performed data analysis and OR designed the study, carried out experiments and wrote the paper.

Acknowledgements

This study was funded by an ERC advanced grant number: 232816 and RANNIS grant number: 130591-053. The authors would like to thank Bjarni Asgeirsson at the Icelandic Science Institute for help with ITC and Athel-Cornish Bowden for his help and support in data analysis. The authors would also like thank the reviewers for critically reading the manuscript and providing helpful comments.

Figures

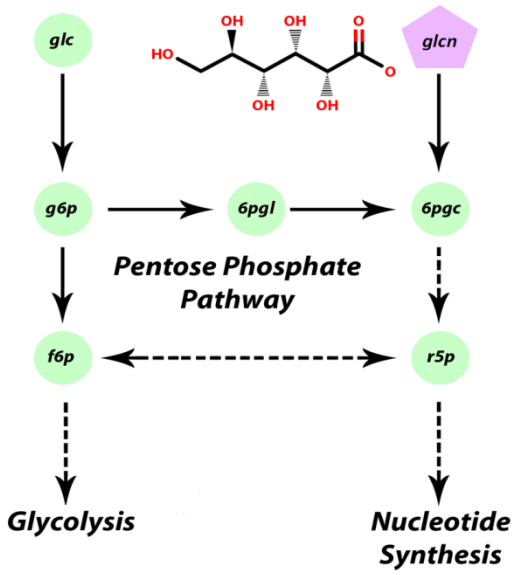

Fig. 1. Overview of the gluconate metabolism in humans. Gluconate is phosphorylated by gluconokinase (EC 2.7.1.12). 6-phosphogluconate can then be degraded through the pentose phosphate pathway although the biological context in which this occurs in humans has not been demonstrated.

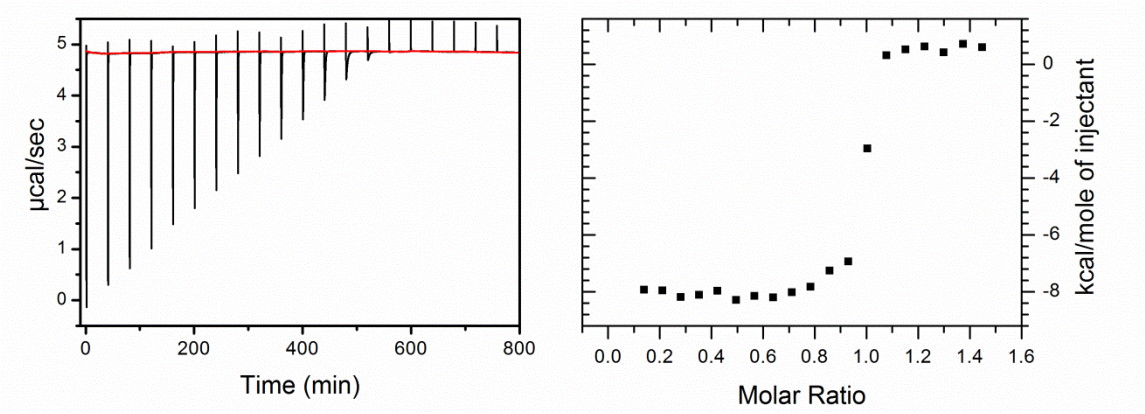

Fig. 2. Micro-calorimetric titration isotherm for determination of enthalpy of the hGntK reaction. Injections of 0.7 µL gluconate (20 mM) were done every 40 minutes, into a cell containing hGntK (33.5 nM) and an excess of ATP (1 mM). Each peak in the left graph corresponds to the heat released on addition of gluconate to the reaction cell. The total heat accumulated up to a particular injection is normalized to the total gluconate concentration at that step and is plotted against the ratio of the total gluconate concentration at that step to the total ATP concentration. This yields the titration curve shown in the right graph. The

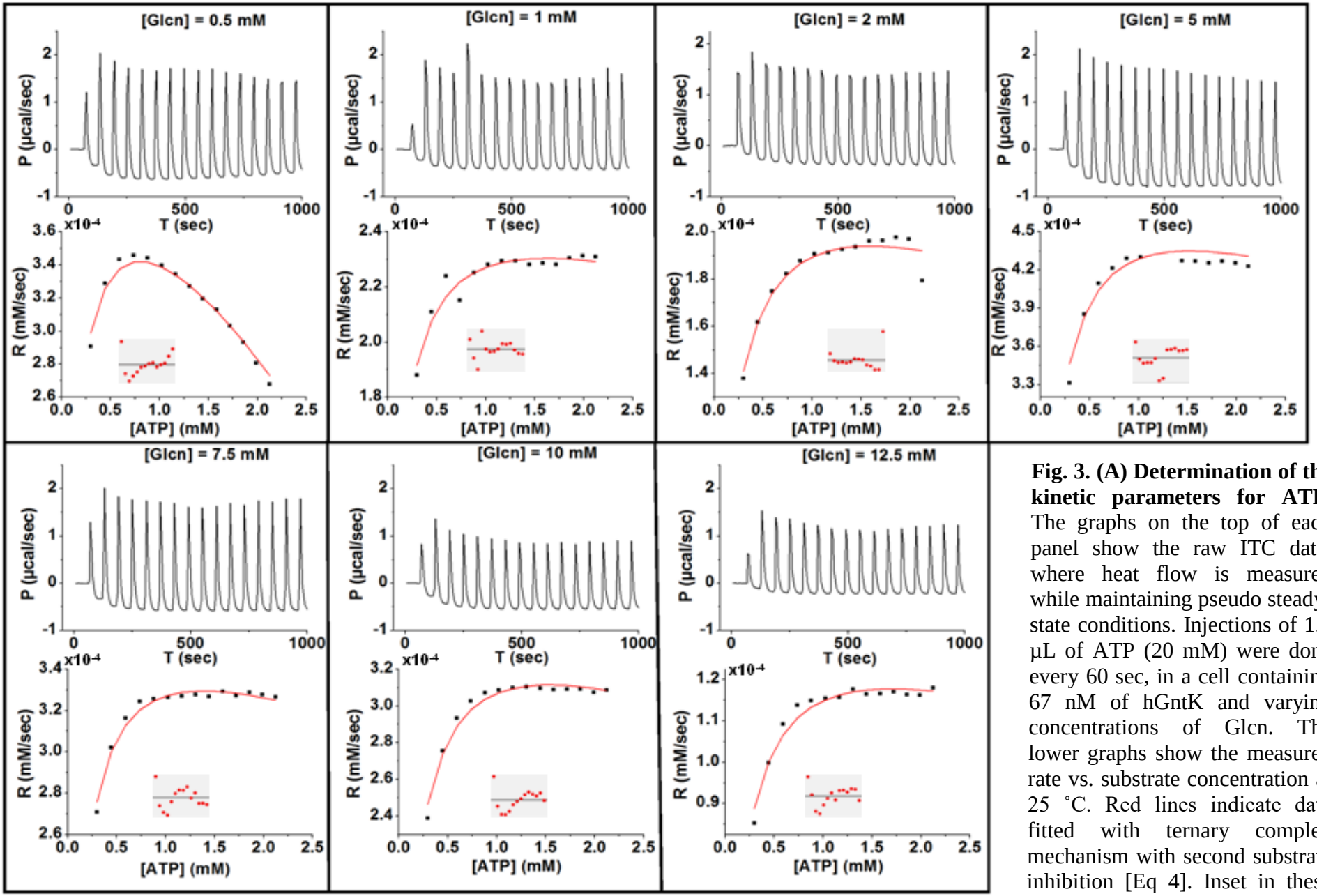

Fig. 3. (A) Determination of the kinetic parameters for ATP. The graphs on the top of each panel show the raw ITC data, where heat flow is measured while maintaining pseudo steady-state conditions. Injections of 1.5 µL of ATP (20 mM) were done every 60 sec, in a cell containing 67 nM of hGntK and varying concentrations of Glcn. The lower graphs show the measured rate vs. substrate concentration at 25 ˚C. Red lines indicate data fitted with ternary complex mechanism with second substrate inhibition [Eq 4]. Inset in these graphs show the residuals from the fitting procedure.

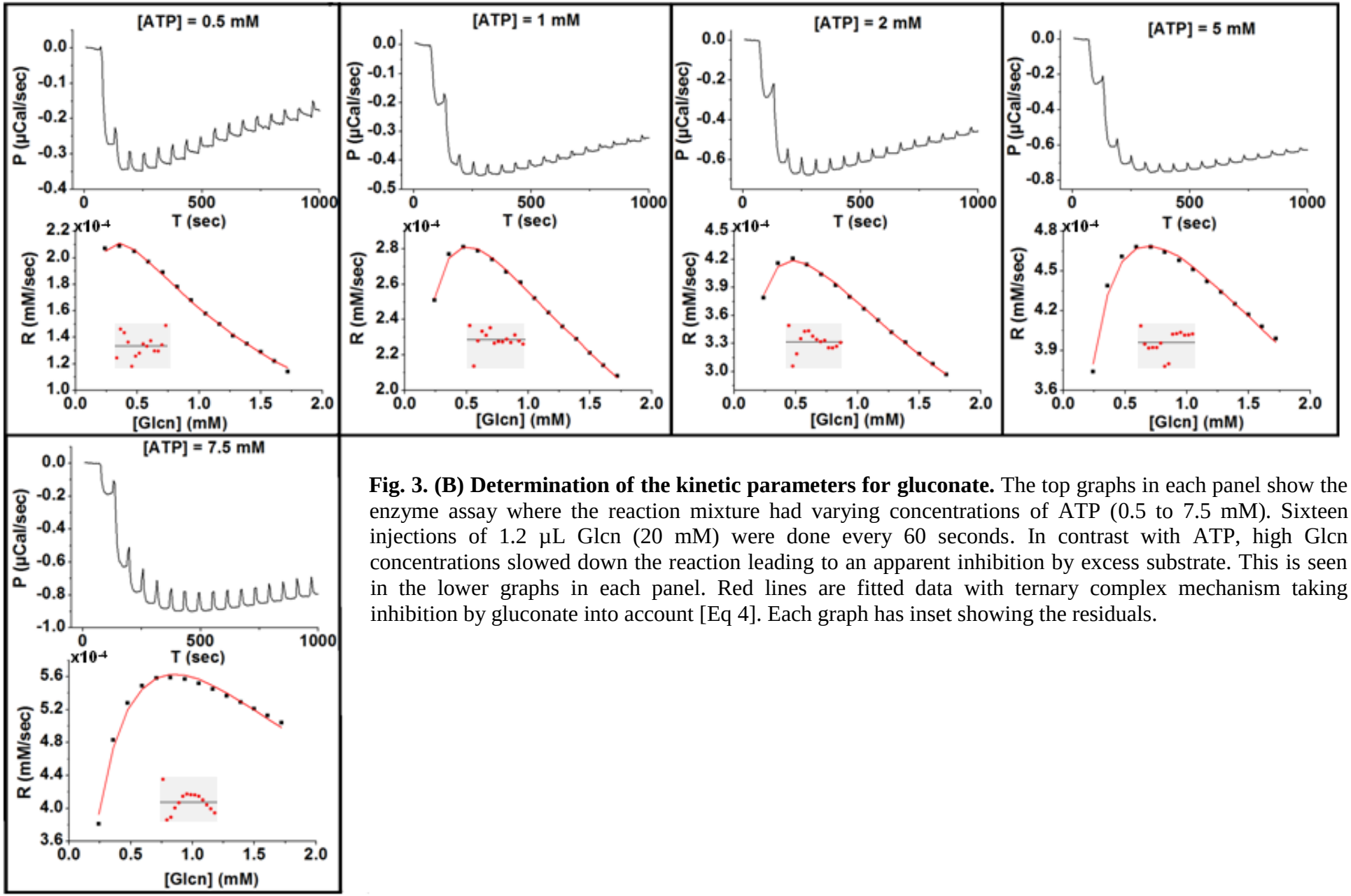

Fig. 3. (B) Determination of the kinetic parameters for gluconate. The top graphs in each panel show the enzyme assay where the reaction mixture had varying concentrations of ATP (0.5 to 7.5 mM). Sixteen injections of 1.2 µL Glcn (20 mM) were done every 60 seconds. In contrast with ATP, high Glcn concentrations slowed down the reaction leading to an apparent inhibition by excess substrate. This is seen in the lower graphs in each panel. Red lines are fitted data with ternary complex mechanism taking inhibition by gluconate into account [Eq 4]. Each graph has inset showing the residuals.

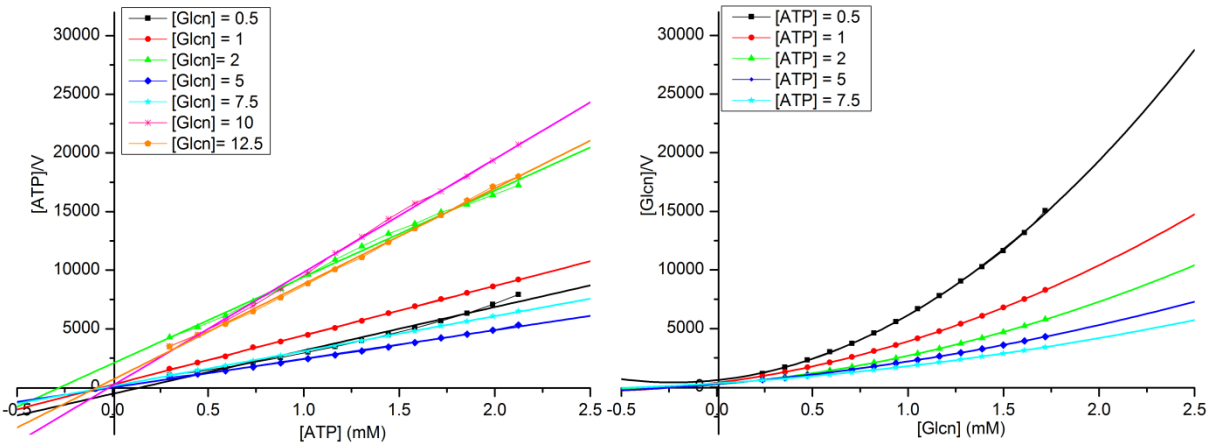

Fig. 4. Hanes-Woolf plots of hGntK catalyzed reaction at altering Glcn and ATP concentrations. (A) For ATP at fixed concentrations of Glcn 0.5 mM (black; square), Glcn 1 mM (red; circle), 2 mM (green; triangle), 5 mM (blue; diamond), 7.5 mM (cyan; star), 10 mM (magenta; star), 12.5 mM (orange; pentagon). The curves are linear and do not have a common point of intersection. **(B)** Analogous plots for Glcn at fixed concentrations of ATP: 0.5 mM (black; square), 7.5 mM (cyan; star), 10 mM (magenta; star). The curves here are parabolic in contrast to the first graph and have a single intersection point. These two graphs together, point towards a ternary complex mechanism, with Glcn inhibition.

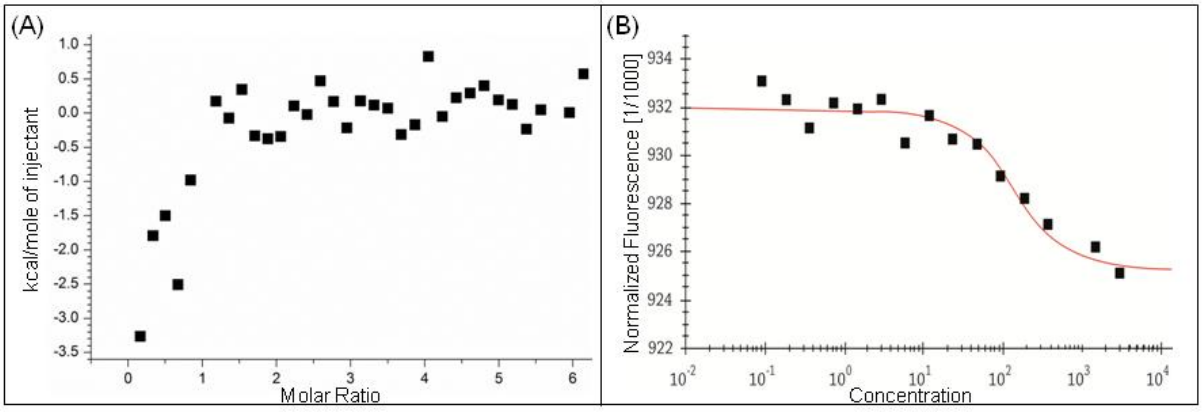

Fig. 5. (A) Binding of ATP and hGntK. Left graph is a thermogram showing the binding of ATP to the enzyme. 36 injections of 1 µL of ATP (1 mM) were done every 120 seconds, into a cell containing 52.3 µM of hGntK (4 outlier data points were removed) **(B) Binding of ATP and hGntK (MST).** Concentrations on the horizontal axis are plotted in µM, with normalized fluorescence on the vertical axis. A K_d of 90.5 µM +/- 9.5 µM was determined for this interaction. For Glcn binding to hGntK in the absence of ATP, binding detected was too low.

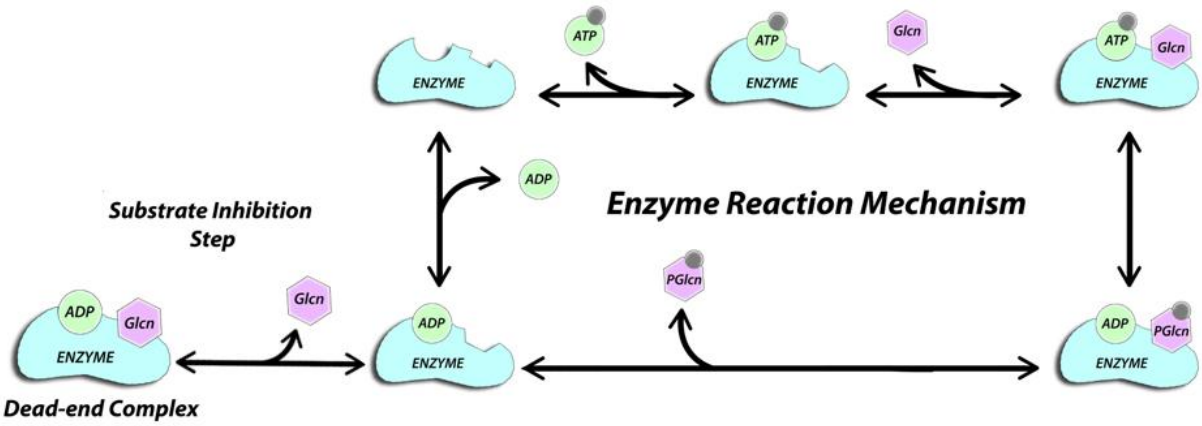

Fig. 6. Proposed mechanism of hGntK catalysis (Start from top left). The reaction follows a compulsory-order ternary-complex mechanism, with ATP binding first. Glcn then binds to form 6-pglcn. Glcn also binds to the Enzyme-ADP complex to form a non-productive dead-end complex, which results in reduction of the reaction rate.

	k_{cat} (sec^{-1})	K_MA (mM)	Residual error
[Glcn] = 0.5 mM	14.95 ± 9.28	0.16 ± 0.04	0.002109
[Glcn] = 1 mM	9.75 ± 1.65	0.28 ± 0.11	0.000333
[Glcn] = 2 mM	8.95 ± 2.78	0.89 ± 0.80	0.000351
[Glcn] = 5 mM	9.35 ± 1.46	0.12 ± 0.01	0.003564
[Glcn] = 7.5 mM	9.17 ± 3.78	0.11 ± 0.02	0.000681
[Glcn] = 10 mM	5.47 ± 0.39	0.20 ± 0.07	0.000466
[Glcn] = 12.5 mM	6.38 ± 2.02	0.30 ± 0.16	0.001012

Table1. Kinetic parameters for ATP. The parameter values are obtained by fitting measurements to Eq. 4 (**Fig. 3A)**. The values listed are average ± standard deviation from three replicates.

	k_{cat} (sec^{-1})	K_MG (mM)	K_{si} (mM)	Residual error
[ATP] = 0.5 mM	15.08 ± 3.60	0.33 ± 0.09	0.38 ± 0.13	0.000082
[ATP] = 1 mM	15.47 ± 6.38	0.20 ± 0.02	1.15 ± 0.45	0.000049
[ATP] = 2 mM	14.69 ± 2.14	0.16 ± 0.02	1.52 ± 0.23	0.000116
[ATP] = 5 mM	15.64 ± 1.38	0.22 ± 0.02	2.85 ± 0.55	0.000781
[ATP] = 7.5 mM	16.01 ± 4.51	0.34 ± 0.03	2.30 ± 0.62	0.000766

Table2. Kinetic parameters for Glcn. The parameter values are obtained by fitting measurements to Eq. 4 (**Fig. 3B)**. The values listed are average ± standard deviation from three replicates.

References

1. Ramachandran, S., Fontanille, P., Pandey, A., & Larroche, C. (2006). Gluconic acid: properties, applications and microbial production. *Food Technology and Biotechnology*, *44*(2), 185-195.
2. Singh, O. V., & Kumar, R. (2007). Biotechnological production of gluconic acid: future implications. *Applied microbiology and biotechnology*, *75*(4), 713-722.
3. Psychogios, N., Hau, D. D., Peng, J., Guo, A. C., Mandal, R., Bouatra, S., *et al.* (2011). The human serum metabolome. *PloS one*, *6*(2), e16957.
4. Bouatra, S., Aziat, F., Mandal, R., Guo, A. C., Wilson, M. R., Knox, C., *et al.* (2013). The human urine metabolome. *PloS one*, *8*(9), e73076.
5. Ottar, R., Giuseppe, P., Manuela, M., Bernhard, O. P., & Ines, T. (2013). Inferring the metabolism of human orphan metabolites from their metabolic network context affirms human gluconokinase activity. *Biochemical Journal*,*449*(2), 427-435.
6. Salvemini, F., Franzé, A., Iervolino, A., Filosa, S., Salzano, S., & Ursini, M. V. (1999). Enhanced glutathione levels and oxidoresistance mediated by increased glucose-6-phosphate dehydrogenase expression. *Journal of Biological Chemistry*, *274*(5), 2750-2757.
7. Riganti, C., Gazzano, E., Polimeni, M., Aldieri, E., & Ghigo, D. (2012). The pentose phosphate pathway: an antioxidant defense and a crossroad in tumor cell fate. *Free Radical Biology and Medicine*, *53*(3), 421-436.
8. Rohatgi, N., Nielsen, T. K., Bjørn, S. P., Axelsson, I., Paglia, G., Voldborg, B. G., *et al.* (2014). Biochemical characterization of human gluconokinase and the proposed metabolic impact of gluconic Acid as determined by constraint based metabolic network analysis.
9. Stetten, M. R., & Topper, Y. J. (1953). Pathways from gluconic acid to glucose in vivo. *Journal of Biological Chemistry*, *203*(2), 653-664.
10. Peekhaus, N., & Conway, T. (1998). What's for dinner?: Entner-Doudoroff metabolism inEscherichia coli. *Journal of bacteriology*, *180*(14), 3495-3502.
11. Zhang, Y., Zagnitko, O., Rodionova, I., Osterman, A., & Godzik, A. (2011). The FGGY carbohydrate kinase family: insights into the evolution of functional specificities.
12. Tong, S., Porco, A., Isturiz, T., & Conway, T. (1996). Cloning and molecular genetic characterization of the Escherichia coli gntR, gntK, and gntU genes of GntI, the main system for gluconate metabolism. *Journal of bacteriology*,*178*(11), 3260-3269.
13. Kraft, L., Sprenger, G. A., & Lindqvist, Y. (2001). Crystallization and preliminary X-ray crystallographic studies of recombinant thermoresistant gluconate kinase GntK from Escherichia coli. *Acta Crystallographica Section D: Biological Crystallography*, *57*(8), 1159-1161..
14. Kraft, L., Sprenger, G. A., & Lindqvist, Y. (2002). Conformational changes during the catalytic cycle of gluconate kinase as revealed by X-ray crystallography. *Journal of molecular biology*, *318*(4), 1057-1069.
15. Chakrabarti, A., Miskovic, L., Soh, K. C., & Hatzimanikatis, V. (2013). Towards kinetic modeling of genome-scale metabolic networks without sacrificing stoichiometric, thermodynamic and physiological constraints. *Biotechnology journal*, *8*(9), 1043-1057.
16. Pace, C.N., et al., *How to Measure and Predict the Molar Absorption-Coefficient of a Protein.* Protein Science, 1995. **4**(11): p. 2411-2423.
17. Wiseman, T., Williston, S., Brandts, J. F., & Lin, L. N. (1989). Rapid measurement of binding constants and heats of binding using a new titration calorimeter. *Analytical biochemistry*, *179*(1), 131-137.
18. Haq, I., & Hill, B. (2002). Calorimetry in the fast lane: The use of ITC for obtaining enzyme kinetic constants. *Microcal, LLC application note*.
19. Bianconi, M. L. (2007). Calorimetry of enzyme-catalyzed reactions. *Biophysical chemistry*, *126*(1), 59-64.
20. Todd, M. J., & Gomez, J. (2001). Enzyme kinetics determined using calorimetry: a general assay for enzyme activity?. *Analytical biochemistry*,*296*(2), 179-187.

21. Freyer, M. W., & Lewis, E. A. (2008). Isothermal titration calorimetry: experimental design, data analysis, and probing macromolecule/ligand binding and kinetic interactions. *Methods in cell biology*, *84*, 79-113.
22. Cornish-Bowden, A. (1995). Briefly Noted. Fundamentals of Enzyme Kinetics, revised edition. *Analytical Biochemistry*, *231*(1), 275.
23. Bianconi, M. L. (2003). Calorimetric determination of thermodynamic parameters of reaction reveals different enthalpic compensations of the yeast hexokinase isozymes. Journal of Biological Chemistry, 278(21), 18709-18713.
24. Coffee, C. J., & Hu, A. S. L. (1972). The kinetic characterization of gluconokinase from a pseudomonad. *Archives of biochemistry and biophysics*,*149*(2), 549-559.
25. Tsai, C. S., Shi, J. L., & Ye, H. G. (1995). Kinetic studies of gluconate pathway enzymes from Schizosaccharomyces pombe. *Archives of biochemistry and biophysics*, *316*(1), 163-168.
26. Heavner, B. D., & Price, N. D. (2015). Transparency in metabolic network reconstruction enables scalable biological discovery. *Current opinion in biotechnology*, *34*, 105-109.
27. Shlomi, T. (2009). Metabolic network-based interpretation of gene expression data elucidates human cellular metabolism. *Biotechnology and Genetic Engineering Reviews*, *26*(1), 281-296.
28. Ruppin, E., Papin, J. A., De Figueiredo, L. F., & Schuster, S. (2010). Metabolic reconstruction, constraint-based analysis and game theory to probe genome-scale metabolic networks. *Current opinion in biotechnology*, *21*(4), 502-510.
29. Campoy, A. V., & Freire, E. (2005). ITC in the post-genomic era…? Priceless.*Biophysical chemistry*, *115*(2), 115-124.
30. Bertalanffy, L. V. (1968). *General system theory: Foundations, development, applications* (p. XV). New York: Braziller.
31. Fleming, R. M., & Thiele, I. (2011). von Bertalanffy 1.0: a COBRA toolbox extension to thermodynamically constrain metabolic models. *Bioinformatics*,*27*(1), 142-143.